Optimising structural loading and power production for floating wave energy converters

Leah Barker Ewart[#1], Philipp R. Thies[2], Tim Stratford[3], Nigel Barltrop[4]

[#]*Industrial Doctorate Centre for Offshore Renewable Energy (IDCORE), University of Strathclyde*
[1]l.ewart@ed.ac.uk

[2]*University of Exeter*
[3]*University of Edinburgh*
[4]*University of Strathclyde*

Abstract— **This paper investigates the design trade-off between power production and structural loading for Wave Energy Converters (WECs), based on tank test results for the Albatern 12S floating wave energy array. This work feeds into the design development process, which is currently in the concept design and testing phase. The paper focuses on two methods for reducing structural loading: limiting the power take off (PTO) torque generation capacity (for operational loads), and controlling the PTO damping (for extreme loads).**

The torque that can be generated by the primary PTO mechanism affects the size (and cost) of the structural components within the device. Increased torque results in a potentially greater power capture, but also greater structural loading. It is therefore important to highlight the target torque limit early in the design process. The aim of this work is to identify the optimum torque limit to refine the design towards the lowest overall Levelised Cost of Energy (LCoE). In addition, a high-level investigation of the impact of PTO damping on extreme loading has been carried out, to help to identify appropriate "operational" and "survival" sea states for the device.

The paper calculates an optimum torque limit for the device at the West Harris site and quantifies the trade-off between Annual Energy Production and structural cost, using the LCoE as an optimisation criteria. The approach is in principle applicable to other technologies, if the design drivers are adjusted to the technology's working principle.

Keywords— **Wave energy, structural loading, tank testing, power production, LCoE.**

I. Introduction

During the early developmental stages of a wave energy converter (WEC), the primary research focus is the power production potential of the device, with optimisation of the structural design being a secondary concern. However, to progress beyond the development phase and move towards commercialisation, a more holistic view is required, with greater consideration of all factors that contribute the overall levelised cost of energy (LCoE).

Maximising power production across all sea states can increase the overall opportunities for revenue generation. However greater power production results in larger loads applied to the structure and the power take off (PTO) system, which in turn increases the cost of the device components. It is therefore important to consider the trade-off between maximising power production and minimising structural loading at an early developmental stage to ensure that it is possible to design a reliable and robust WEC structure, while achieving an acceptable LCoE.

This paper investigates this design trade-off for the Albatern 12S WEC, using results from tank testing carried out in the Flowave Ocean Energy Research Facility. The tank test set up is covered in Section II.

Two approaches to load limitation are covered in this study:

1) *PTO Torque Limitation:* The power generation capability of a device is limited by the amount of torque that can be generated by the power take off (PTO) mechanism. The effect of limiting the PTO torque on operational loads is investigated to identify the optimum torque limit which results in the lowest LCoE. The methodology is discussed in section III, with the results presented in sections IV.
2) *PTO damping control:* During operation, power output and structural loads will vary depending on the level of PTO damping. Damping can be controlled throughout operation to maximise power output in frequently occurring seas, and shed load in storm conditions. The effect of PTO damping control is considered in Section V, and the potential impact on extreme loads is discussed.

II. Tank Testing Set Up

The Albatern 12S device is a multi-body floating wave energy converter, consisting of node and link elements which can be configured in different numbers to form an array (Fig 1).

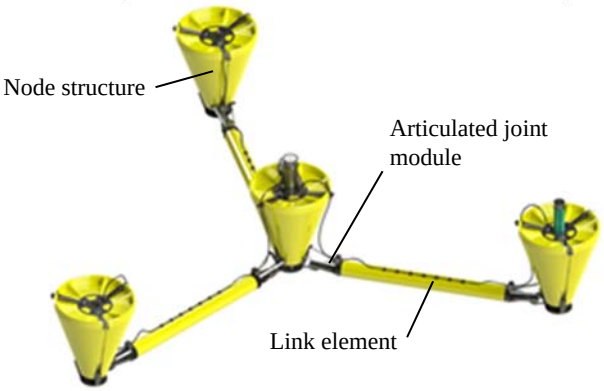

Fig. 1 Albatern 12S multi-body floating wave energy converter schematic

Fig. 1 shows the schematic of a system of 4 nodes and three link arms. Testing was carried out on a "1 Hex" array, consisting of 9 nodes, and 18 link elements (Fig. 2 and 3).

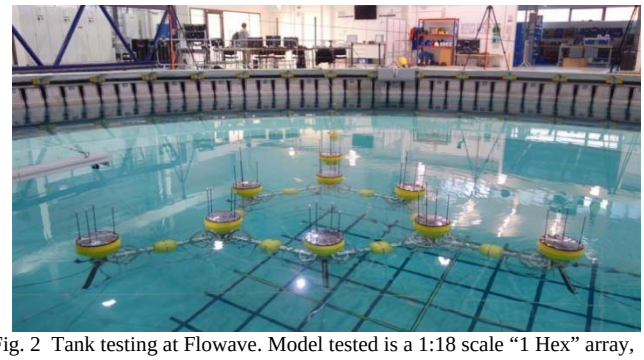

Fig. 2 Tank testing at Flowave. Model tested is a 1:18 scale "1 Hex" array, with 9 node and 18 link elements.

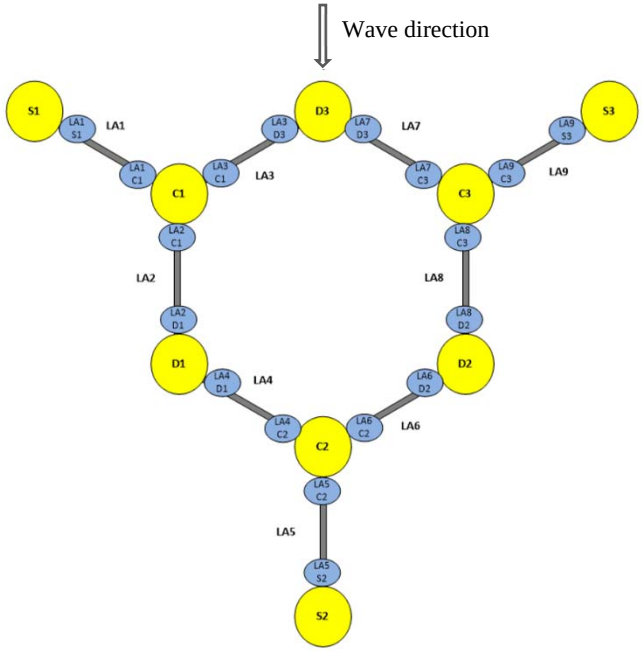

Fig. 3 Test array schematic and naming convention

A. PTO simulation

The Albatern device converts the incoming wave energy into mechanical power via the PTO mechanism at each joint which damps the relative motion of the node and link. Mechanical power capture is equal to the PTO torque (T) multiplied by the joint angular velocity (ϖ), and the generated torque is directly related to the PTO damping characteristics.

Details of the full-scale PTO mechanism are still in development; however, the main design criterion is to provide damping (and therefore power take off) around three degrees of freedom at each joint (as shown in Fig 4). This behaviour has been replicated at model scale using multiple high torque DC brushless Maxon motors. Each link arm contains five motors – two at each end resisting the motion in the pitch and yaw axis, and one in the centre resisting motion around the torsion axis. Each motor is controlled by an Escon drive, allowing for individual control of five degrees of freedom per link arm (45 in total for the whole model). The drive allows the PTO damping to be actively controlled using a feedback control loop, which provides an appropriate current to the motor based on the instantaneous measured angular velocity. Output motor torque is directly proportional to the motor current, and therefore it is possible to provide a specified torque for a given articulation velocity. Linear damping was applied during testing, whereby the output torque (T) was linearly proportional to the measured angular velocity (ϖ), however it would be possible with this system to test much more complex control strategies.

To provide the required torque at the pitch and yaw axis, wire drive gearing mechanisms are used, with sector arcs to ensure linearity between the motor and axis responses, (Fig. 4). The wire lies along the arcs and is wrapped around the motor shaft to drive the motor. A mechanical gearbox is used in conjunction with the torsion motor to provide the required torque in this axis.

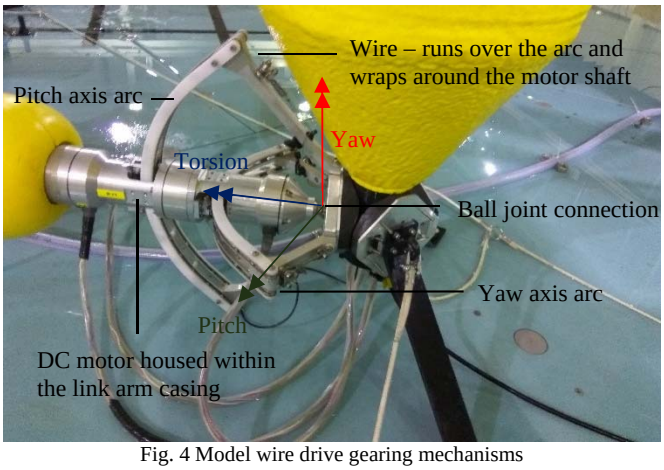

Fig. 4 Model wire drive gearing mechanisms

B. Load measurement

During testing, articulation torques were measured at the pitch and yaw axis using submersible inline tension load cells (manufactured by Applied Measurements, with a 0-50N measurement range) attached to the wire drive gear mechanism (Fig. 5).

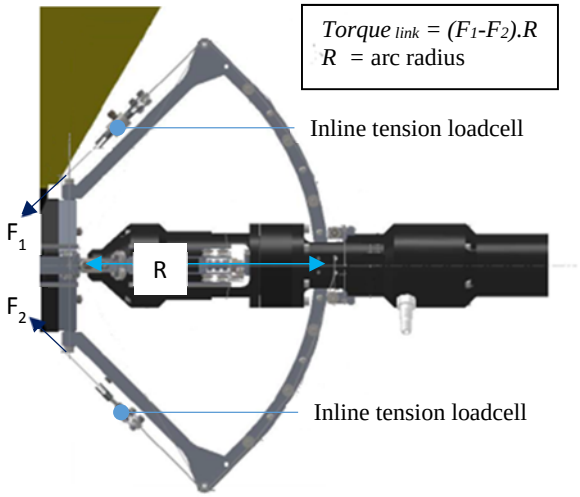

Fig. 5 Link arm end torque measurement

Unfortunately, due to budgetary constraints, it was not possible to include two load cells at each articulation axis. The maximum torques occur on the pitch axis on link arms that are in line with the direction of the oncoming waves (LA2, LA8 and LA5 in Fig. 3). Therefore, two load cells were included at the articulation points on these links, to allow accurate measurement of the maximum loads. A single cell was included on each of the other articulation locations, allowing an estimation of the torques to be calculated at these points, to be derived using information about the joint behaviour based on the articulations with the double load cells.

Link arm torsion moments were measured using a torsion load cell, placed in the centre of the link, manufactured by Futek, with a 0-5.65Nm measurement range.

C. Power capture

Two different methods have been used to measure the electrical and mechanical power captured in the array. The electrical power of the motors is calculated from direct measurements of the motor current and angular velocity, as shown in the following equations:

$$Torque_{motor} = C_t.I_m \qquad Power_{motor} = Torque_{motor}.\omega_m$$

(C_t =torque constant, I_m = current, ω_m = angular velocity).

Mechanical power has been calculated using the direct measurements of torque using the inline load cells, together with the angular velocity of the motor:

$$Power_{mech} = Torque_{link}.\omega_m$$

As an accurate measurement of the mechanical power is only possible at the articulations with two load cells, the total power capture by the array reported here is the sum of the measured mechanical power for the inline pitch articulations, and the electrical power of all other articulation locations.

Mechanical power capture is greater than the electrical power capture due to losses in the system associated with the PTO model set up, therefore this method for calculating total power capture is conservative in terms of mechanical power capture and optimistic regarding electrical power capture. While it would be possible to make a more accurate assessment of the mechanical power using data from the single load cells, at the time of writing this analysis had not been done. However, this is acceptable for this study as power output values are used for comparison only, and therefore accurate assessment of the absolute values is not necessary.

D. Test Sea States

The device was tested in 11 regular sea states (Table I), and 21 irregular sea states (Table II).

TABLE I
REGULAR TEST SEA STATES, REPORTED VALUES AT FULL SCALE

H(m) / T(s)	5.5	6.5	7.5	8.5	9.5	10.5
4.5			x			
3.5		x	x	x		
2.5			x			
1.5	x	x	x	x	X	X

TABLE II
IRREGULAR TEST SEA STATES (JONSWAP, GAMMA = 1)
REPORTED VALUES AT FULL SCALE

Hs (m) / Tp (s)	7.7	9.1	9.9	10.5	11.9	12.6	13.3	14.7
4.5				**x**	**x**			
4								
3.5		x		x			x	
3			x			x		
2.5	x		x			x		
5	x	x		x		x		
1.5	x	x		x			x	x
1	x		x					

Following guidance in [1], lines of constant significant wave height and peak period are included, as this allows the results to be extrapolated with some degree of confidence to give power output for all elements of the bivariate H_s / T_p wave occurrence matrix.

E. Damping Optimisation

As discussed in II.A, the motors were controlled to provide linear damping during testing. Tests were carried out with different applied damping levels to identify the optimum damping value for power output. The torsion damping was held at a constant value, and the pitch and yaw damping was varied between 500-6000 kNms/rad (full-scale). The full power matrix was then built up using the damping value which gave the highest power output at each sea state. In general, higher damping values were optimum for larger, steeper waves, with lower values giving higher power output for shallower, longer period waves. All power matrices discussed in this paper are based on the optimum damping levels for each sea state.

III. PTO Torque Limitation: Optimisation Methodology

This section investigates the impact of limiting the PTO torque generation capacity on power output, structural loading, and LCoE.

A. Power Output

In the scale model, the DC motors were sized to ensure that there were no constraints on the torque generated during testing. However in reality, there will be a limitation on the torque that can produced by the full-scale PTO mechanism. The amount of torque that can be achieved affects both the sizing and cost of the PTO components, as well as the sizing of the structural components, as this is one of the primary loads acting on the device. Therefore, setting the target PTO torque is an important design decision that needs to be made at an early point in the design process.

The effect of limiting the torque on overall power production has been investigated by post-processing the tank testing results. For each test sea state, the measured torque has been capped at the specified torque limit; this capped torque has then been used to recalculate the mean power capture (see Section II.C). It is noted that this is not entirely accurate as a physical torque limit would alter the behaviour of the device. However, at this stage this estimation is used to indicate the potential optimum torque limit, as including multiple torque limits within the physical testing would significantly increase the required testing time.

An example of the post-processed torque limited time history compared with the actual measured torque is shown in Fig. 6, for the case where torque is limited at 600kNm (full scale).

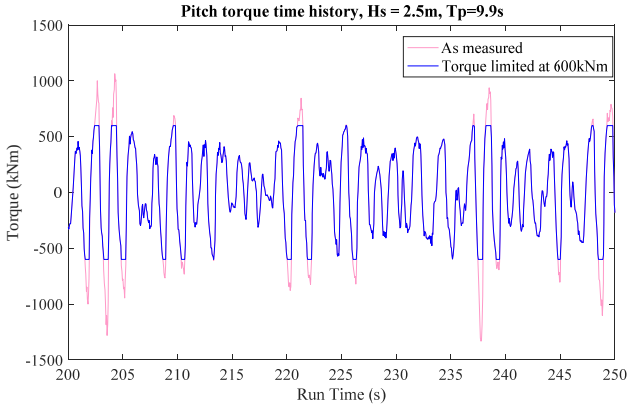

Fig. 6 Torque limited time history (Torque reported at Full Scale)

The post-processed results have then been used to develop a full power matrix for each specified torque limit. Data has been interpolated and extrapolated using the scatteredInterpolant data object in Matlab. There is some uncertainty associated with the results using this method, however as the tests cover the most commonly occurring sea states, the level of uncertainty is acceptable for comparison between different torque limits.

The power matrix has been combined with the occurrence matrix for a location to the west of the Isle of Harris to give an estimate of the Annual Energy Production (AEP). The West Harris site is a potential location for commercial deployment of the device, and occurrence data has been provided by MetOcean Solutions

B. PTO Sizing

While the exact details of the full-scale PTO mechanism are still in development, the high-level concept is to have two hydraulic cylinders attached to the node and link using ball joints, allowing for movement and damping around three axes (Fig. 7).

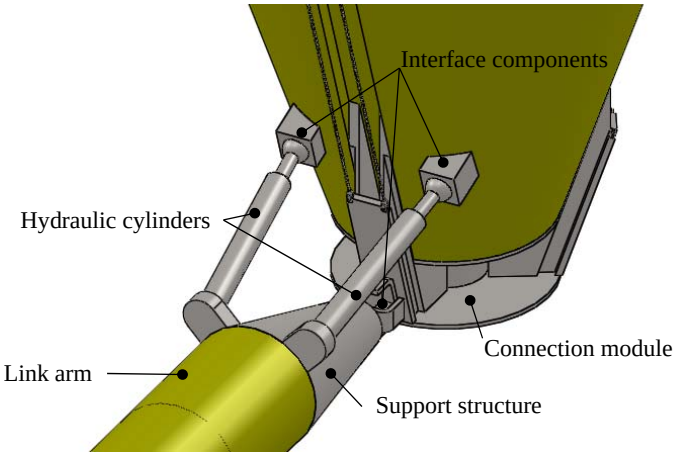

Fig. 7 High level concept for PTO mechanism

Assuming an operating pressure of 250bar for the cylinders, the required cylinder bore size has been calculated to give the appropriate ram force for a given torque limit as shown in Fig. 8.

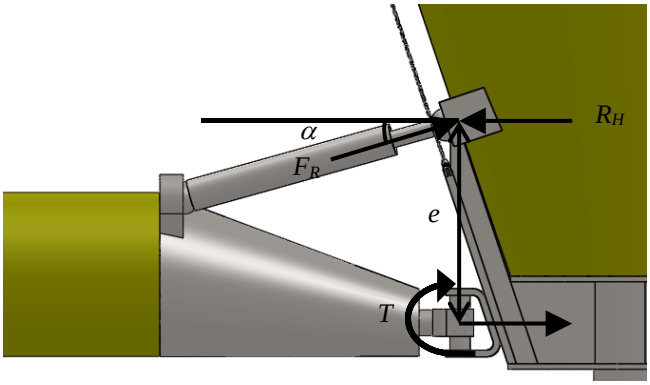

Fig. 8 Calculation of required cylinder bore for given PTO torque

PTO torque:	T	
Eccentricity:	e	$= 1.5m$
Angle:	a	$= 20^o$
Reaction force:	R_H	$= T/e$
Cylinder pressure:	P	$= 250bar$
Bore:	B	
Cross sectional area:	A	$= B^2\pi/4$
Ram force:	F_R	$= PA = R_H/cos\alpha$

C. Structural Design

For identification purposes, the device components are categorised into different systems and sub-systems as shown in Table III. This table also lists the components that are relevant to the structural design; these are shown in Fig.7.

TABLE III
SYSTEMS, SUBSYSTEMS AND COMPONENTS OF ALBATERN 12S ARRAY

SYSTEM / subsystem / *component*
STRUCTURAL SYSTEM
Node module
Link element
Link arm steel tube
Fixtures and fittings
Joint module
Hydraulic cylinder
Support structure
Interface components
Fixtures and fittings
Connection module
MECHANICAL & ELECTRICAL
MOORING SYSTEM
TRANSMISSION AND GRID CONNECTION

For this study, it has been assumed that the overall structural requirements can be characterised by the design requirements of the Link arm. This component is to be constructed from a steel tube, and the applied load actions can be directly derived

from the applied PTO torque, independent of the actual configuration of the PTO mechanism.

In contrast the details of the Joint and Connection Module will be very dependent on the PTO mechanism, and therefore outside the scope of this study. At this conceptual stage, it has been assumed that the weight of the steelwork in these components varies in direct proportion to the change in required Link arm weight.

The design of the Node structure will be for the most part driven by wave pressures on the hull (except for the connection to the steelwork), and therefore will not be greatly affected by the PTO torque. It has therefore been assumed that the design of this element is the same for all torque levels.

Structural design of the elements of a WEC should, as far as appropriate, be carried out in accordance with relevant codes and guidelines, such as [2]. This reference sets out the following limit states for design:

- Ultimate Limit State (ULS): corresponding to the ultimate resistance for carrying loads;
- Fatigue Limit State (FLS): related to the possibility of failure due to the effect of cyclic loading;
- Accidental limit states (ALS) corresponding to damage to an accidental event of operational failure;
- Serviceability limit states (SLS) corresponding to the criteria applicable to normal use or durability.

The main purpose of the tank testing was to verify the power output capabilities of the device in operational sea states, and did not include any testing in extreme sea states. It is therefore not possible to derive any ULS or ALS loadcases from the testing results. However, as noted in [3], for dynamic devices such as WECs, fatigue aspects are likely to govern the design. As the 21 irregular test sea states cover 42% of the sea states encountered in each year at the West Harris site, it is possible to estimate the fatigue loading on link arm for a 20-year design life based on the tank testing results.

Fatigue analysis has been carried out for the most heavily loaded link arm at the back of the array (LA5/S2). As this link is in-line with the waves, pitch loading is dominant and yaw and torsion loading are negligible.

Fatigue design has been carried out in accordance with [4], with analysis based on S-N data as set out in this reference. Fatigue damage has been calculated assuming linear cumulative damage (Palmgren-Miner rule), with the accumulated fatigue damage calculated in accordance with the following equation:

$$D = \sum_{i=1}^{k} \frac{n_i}{N_i} = \frac{1}{\bar{a}} \sum_{i=1}^{k} n_i . (\Delta\sigma_i)^m \leq \eta$$

D = accumulated fatigue damage
k = number of stress blocks
n_i = number of stress cycles in stress block i
N_i = number of cycles to failure at constant stress range $\Delta\sigma_i$
a = intercept of the S-N curve with the log N axis
m = negative inverse slope of the S-N curve
η = usage factor =1/DFF
DFF = Design Fatigue Factor

The number of stress cycles (n_i) has been calculated using the post-processed torque time histories from tank testing in irregular waves. Torque cycles have been counted using the rainflow counting method [5], [6], split into blocks with a range of 50kNm. Torque (T) is related to stress in the link arm by the following equation:

$$\sigma = \frac{T}{Z}$$

Z = elastic section modulus = $\frac{(D^4-(D-2.t)^4)}{64}\pi$ for a tube with diameter D and wall thickness t.

Each test time history consists of 10902 readings, with a sampling rate of 20Hz. For the rainflow counting, the first 500 and last 902 reading have been ignored (to allow for warm up and settling time of the tank). Each time history is therefore 475 seconds long at model scale, which relates to a length of 1840s full scale (for an 18th scale model).

To account for the stress cycles encountered over the whole design life of the structure, the number of stress cycles counted within each of the test time histories has been multiplied by an appropriate factor, derived from splitting up the full occurrence matrix. This has been done by assuming that the test sea state results also apply to adjacent sea states. The assumed split applied to the scatter diagram is shown in Fig. 9.

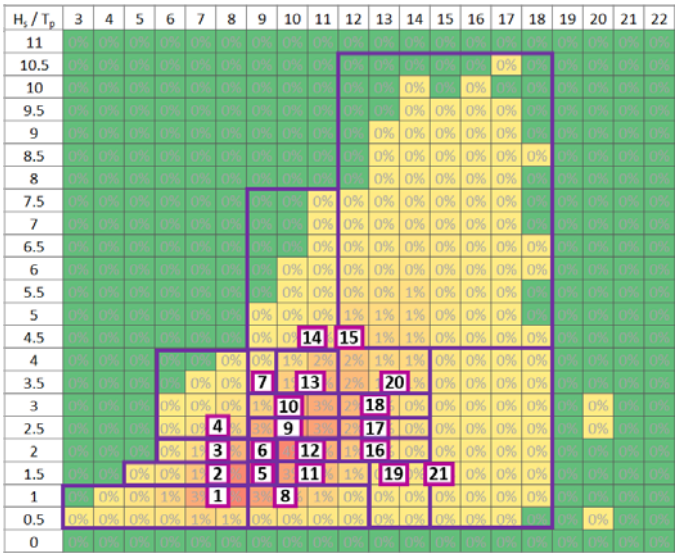

Fig. 9 West Harris wave occurrence matrix, showing the test sea states (numbered), together with the portion of the matrix to which they are assumed to apply.

To calculate N_i for each stress cycle, the link arm has been classified as a "C" fatigue detail, in accordance with Table A.1 of [4], (a rolled steel tube subject to potential rust pitting). For a member in seawater with cathodic protection this gives the following data for the S-N curve (Table 2-2 from [4]):

For N $\leq 10^6$ cycles: $m_1 = 3.0$, log $a_1 = 12.192$

For N $\geq 10^6$ cycles: $m_2 = 5.0$, $\log a_2 = 16.320$

The Design Fatigue Factor has been taken as 1 (from table 5-1 of [2]), as it is assumed that the link arm will be inspected on a regular basis.

D. *Levelised Cost of Energy (LCoE)*

The main aim of this section of work is to select the optimum PTO torque limit which gives the minimum LCoE when considering overall power output and structural costs.

LCoE has been estimated using a tool developed in-house at Albatern. A torque limit of 1MNm has been taken as the baseline scenario. Costs for this scenario were estimated based on discussions with the Albatern design team, bringing together knowledge from production and manufacture of the Albatern prototype 6S device and quotes from suppliers.

The different top level categories that have been considered in the cost estimate are shown in Table IV, together with the % contribution to the total whole life cost.

TABLE IV
CATEGORIES AND CONTRIBUTION TO WHOLE LIFE COST

Category	**% contribution to cost**
Structural system	43.8
Mechanical & electrical system	7.5
Mooring system	12.1
Transmission & grid connection	5.7
Installation	12.3
Operations & Maintenance	18.7

For this paper, it is assumed that all costs remain constant except for the structural components listed in Table III. This is a very simplified assumption, as it is likely that the cost of other components such as hydraulic routing cables and accumulators will also vary with PTO torque. However, any additional increases and decreases are likely to exaggerate any variation in LCoE, and therefore this simplification is acceptable at this level of analysis.

Table V shows the cost of each structural subsystem and component for the baseline scenario as a % of the Structural System cost.

TABLE V
SYSTEMS, SUBSYSTEMS AND COMPONENTS OF ARRAY FOR COST PURPOSES

Subsystem / *component*	**% of structural system cost**
Node	44.5
Link element	16.2
Link arm	*14.7*
Fixtures and fittings	*4.7*
Joint module	39.2
Hydraulic cylinder	*7.6*
Support structure	*11.5*
Interface components	*7.1*
Fixtures and fittings	*3.6*
Connection module	9.6

To estimate the costs for each different torque limit, it is assumed that the cost of the steelwork items (which includes all components listed in Table V, except for the hydraulic rams) vary in proportion with the variation in steel weight of the link arm.

Hydraulic cylinder costs have been estimated based on stock cylinder prices as published on the Interfluid website [7]. A multiplier of 4 has been included in the pricing, to account for the increased cost associated with manufacturing bespoke cylinders; this is based on the difference between the quoted stock price and the actual price paid for the cylinders in the Albatern prototype 6S device. The Interfluid stock cylinders are smaller than those required for the 12S device, but prices increase linearly with bore size and stroke, and therefore the prices have been extrapolated as required.

IV. PTO TORQUE LIMITATION: OPTIMISATION RESULTS

A. *Power Output Results*

Fig. 10 shows the normalised power matrix extrapolated from the unlimited tank testing results over the full range of the West Harris occurrence sea states. Power output is based on the mechanical power capture, and values are given as a percentage of the maximum power output (which occurs when H_s = 10m, and T_p = 11sec).

H_s/ T_p	3	4	5	6	7	8	9	10	11	12	13	14	15	16	17	18	19	20	21
10									100%	95%	92%	89%	86%	82%	71%	60%	58%	56%	54%
9.5									94%	89%	86%	83%	81%	74%	63%	56%	54%	52%	50%
9								92%	88%	83%	80%	78%	75%	66%	56%	52%	50%	48%	46%
8.5								86%	82%	77%	75%	72%	68%	59%	49%	47%	46%	44%	43%
8								80%	76%	72%	69%	66%	60%	51%	45%	43%	41%	40%	40%
7.5							78%	74%	70%	66%	63%	60%	53%	44%	41%	39%	37%	37%	37%
7							72%	68%	64%	60%	58%	54%	46%	39%	37%	35%	35%	34%	34%
6.5							67%	62%	59%	55%	52%	47%	40%	35%	33%	32%	32%	32%	32%
6							66%	56%	53%	49%	46%	40%	33%	31%	29%	29%	29%	29%	29%
5.5						84%	63%	50%	47%	43%	40%	34%	29%	27%	26%	26%	26%	26%	25%
5						79%	59%	45%	41%	37%	34%	28%	25%	24%	23%	23%	23%	23%	22%
4.5					58%	64%	54%	41%	35%	32%	28%	23%	21%	20%	20%	20%	20%	19%	18%
4					46%	52%	48%	35%	29%	26%	22%	19%	18%	17%	17%	17%	16%	16%	15%
3.5					36%	40%	39%	29%	23%	20%	17%	15%	15%	14%	14%	13%	13%	12%	11%
3				31%	30%	31%	30%	19%	18%	15%	12%	12%	11%	11%	10%	10%	9%	9%	8%
2.5				24%	23%	23%	21%	17%	13%	10%	9%	9%	8%	7%	7%	6%	6%	5%	5%
2			28%	24%	20%	16%	13%	11%	8%	6%	5%	5%	5%	4%	3%	3%	2%	2%	1%
1.5			13%	12%	11%	9%	8%	6%	5%	3%	2%	2%	1%	0%	0%	0%	0%	0%	0%
1		9%	8%	6%	5%	3%	2%	2%	1%	0%	0%	0%	0%	0%	0%	0%	0%	0%	0%
0.5	5%	3%	2%	0%	0%	0%	0%	0%	0%	0%	0%	0%	0%	0%	0%	0%	0%	0%	0%

Fig. 10 Extrapolated normalised power matrix based on mechanical power captured during tank testing, for unlimited torque case.

In comparison, as an example, the power matrix for the case where torque has been limited to 600kNm (full scale) is shown in Fig. 11. Values are given as a percentage of the maximum power output for the unlimited torque case shown in Fig. 10.

H_s/ T_p	3	4	5	6	7	8	9	10	11	12	13	14	15	16	17	18	19	20	21
10									78%	76%	74%	72%	70%	67%	62%	56%	54%	53%	51%
9.5									74%	72%	70%	68%	66%	62%	56%	52%	51%	49%	48%
9								72%	70%	67%	65%	63%	61%	56%	51%	49%	47%	46%	44%
8.5								67%	65%	63%	61%	59%	56%	51%	46%	45%	43%	42%	41%
8								63%	61%	58%	56%	54%	51%	46%	43%	41%	40%	39%	38%
7.5							61%	58%	56%	54%	52%	50%	46%	41%	39%	38%	36%	36%	36%
7							56%	54%	52%	50%	47%	45%	41%	37%	35%	34%	33%	33%	33%
6.5							53%	49%	47%	45%	43%	40%	36%	33%	32%	31%	30%	30%	30%
6							52%	45%	43%	41%	38%	35%	31%	30%	28%	28%	27%	27%	27%
5.5						65%	50%	41%	38%	36%	34%	30%	27%	26%	25%	25%	24%	24%	24%
5						61%	47%	37%	34%	32%	29%	26%	24%	23%	22%	22%	21%	21%	21%
4.5					48%	51%	43%	34%	29%	27%	25%	22%	20%	20%	19%	19%	18%	18%	17%
4					39%	42%	38%	29%	25%	23%	20%	18%	17%	17%	16%	16%	15%	15%	14%
3.5					32%	34%	32%	25%	20%	18%	16%	15%	14%	13%	13%	12%	12%	11%	11%
3				28%	27%	27%	25%	17%	16%	14%	12%	11%	11%	10%	10%	9%	9%	8%	7%
2.5				23%	22%	20%	19%	16%	12%	10%	9%	8%	8%	7%	6%	6%	5%	5%	4%
2			27%	23%	19%	15%	13%	10%	8%	6%	5%	5%	4%	4%	3%	3%	2%	1%	1%
1.5			14%	13%	11%	9%	8%	6%	4%	3%	2%	2%	1%	0%	0%	0%	0%	0%	0%
1		9%	8%	6%	5%	3%	2%	2%	1%	0%	0%	0%	0%	0%	0%	0%	0%	0%	0%
0.5	5%	3%	2%	0%	0%	0%	0%	0%	0%	0%	0%	0%	0%	0%	0%	0%	0%	0%	0%

Fig. 11 Extrapolated normalised power matrix based on mechanical power captured during tank testing, for PTO torque limit = 600kNm

Power matrices as shown in Fig. 10 & 11 have been calculated for several different torque limits, and then combined with the West Harris occurrence matrix to calculate the variation in annual mean energy production (AEP), as shown in Fig. 12. It can be seen from this graph that the increase in AEP is significant between 0 and 0.6MNm, but that there is little increase above 1MNm.

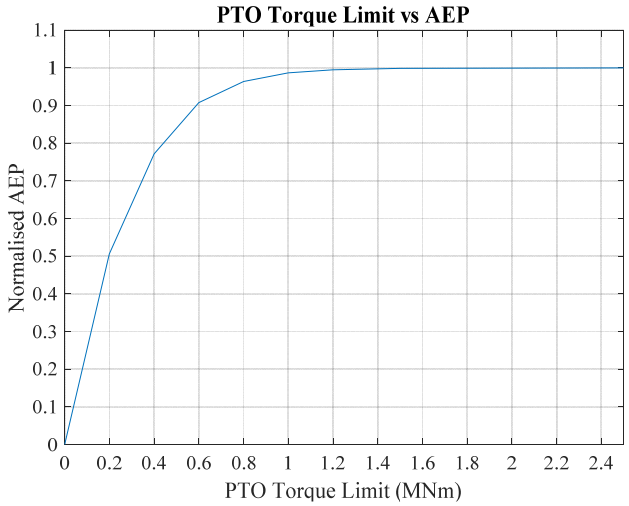

Fig. 12 PTO torque limit (full scale) vs AEP

B. Component Sizing & Costing

1) Hydraulic rams: Table VI shows the required hydraulic cylinder bore size calculated for different PTO torques limits (TL), as described in III.B, together with the estimated cylinder cost.

TABLE VI
HYDRAULIC CYLINDER ESTIMATED SIZE AND COSTS

TL (MNm)	**0.2**	**0.4**	**0.6**	**0.8**	**1**	**1.2**	**1.5**	**2.5**
Bore (mm)	70	100	120	140	160	180	200	250
Cost (1000£)	0.8	1.9	2.5	3	3.5	4.1	4.6	5.9

2) Link Arm: Table VII shows the link arm cross-sectional area (CSA) required to keep fatigue damage accumulation levels below 1 for a life span of 20 years. The table also shows the % variation in required link arm steel weight, when compared to the baseline case.

TABLE VII
REQUIRED LINK ARM CROSS SECTIONAL AREA (CSA)

TL (MNm)	**0.2**	**0.4**	**0.6**	**0.8**	**1**	**1.2**	**1.5**	**2.5**
CSA (cm^2)	50	58	67	79	90	98	102	102
% difference	56	64	74	87	100	109	113	113

3) Device Costs: Cost have been estimated for each of the different torque limits based on the information given in Table VI and VII. For the steelwork items as listed in Table V, it has been assumed that the costs vary in proportion to the required link arm weight.

Fig. 13 shows the variation in costs with PTO torque limit. The Structural costs include all the subsystem as listed in Table V. The total cost includes all systems listed in Table IV (this value was subsequently used to calculate the LCoE) and values have been normalised against the maximum total cost.

These graphs show that generally the structural costs increase with torque limit, however the rate of change slows, with the greatest increase occurring between a torque limit of 0.2 and 1.2MNm. This is because fatigue design is affected by the number of cycles at a particular stress range, not just the magnitude. In any given time period, there will be fewer cycles with larger magnitude loading, and therefore these have less of an impact on the overall design than the smaller magnitude loads, which contribute to a larger proportion of the overall damage. Lower torque limits therefore have a much greater impact on the number of cycles that the structure must endure than the larger torque limits, as they reduce the number of the low stress cycles applied to the device over its lifetime.

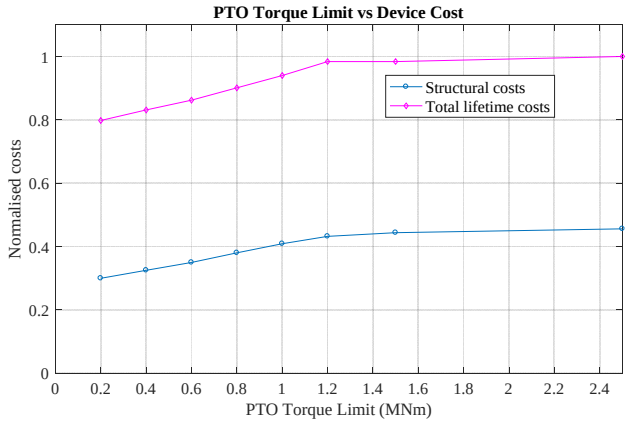

Fig. 13 PTO torque limit (full scale) vs Device Cost to satisfy fatigue design life of 20 years at West Harris site

C. LCoE

LCoE is a function of both device cost and total power production. Fig. 14 shows the variation in cost, AEP and LCoE with PTO torque limit– normalised so that the maximum value of each is taken as 1. It can be seen from this figure that AEP increases rapidly between a torque limit of 0.2 and 0.6 but tends to a limit at around 1.2MNm. Costs continue to increase, but the rate of change slows above 1.2MNm. LCoE therefore shows a significant decrease up to the torque limit of 0.6MNm, and reaches a minimum at 0.8MNm. LCoE then starts to increase again, but at a slower rate than one might instinctively expect, because the rate of cost increase also slows. It should be noted however that this analysis only considers the variation in the cost of the structural items. As noted previously there are likely to be other components which vary in cost with PTO torque, however these differences would likely exaggerate the increase in LCoE for torque limits greater than 0.8kNm, and therefore would not change the overall outcome of the analysis.

This work therefore shows that a torque limit of 0.8MNm would be beneficial, as it results in the lowest LCoE.

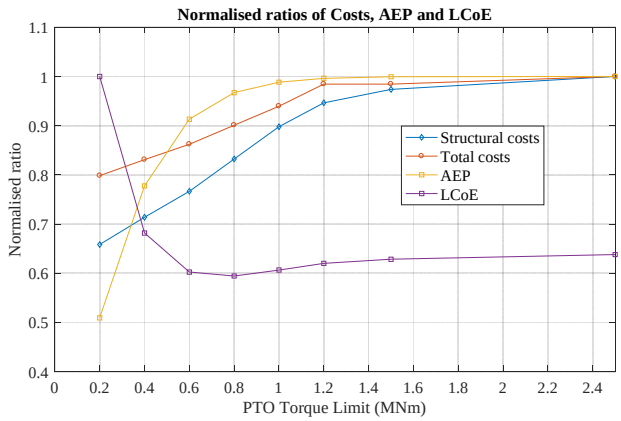

Fig. 14 PTO torque limit (full scale) vs Costs, AEP, and LCoE to satisfy fatigue design life of 20 years at West Harris site

V. PTO Damping Control in Extreme Sea States

While the PTO torque limit is a physical constraint that cannot be changed once the device is built, the PTO damping can be varied throughout the life of the device. During the most frequently occurring sea states the damping should be controlled to give the maximum power output. Higher damping levels however result in greater loads, and therefore it may be possible to reduce the damping in more extreme seas to limit the impact on the structure.

While it is not possible at this stage to determine a detailed PTO damping control strategy, the test results do show that reducing damping levels has a significant effect on the peak bending moment experienced by the link arm as shown in Fig. 15. This shows the pitch moment response for a unit wave height across a range of frequencies for different PTO damping levels as measured during the regular wave tests. It can be seen from this figure that the peak load response for a damping level of 500kNms/rad is nearly 40% less than the peak load response for a damping level of 6000kNms/rad, indicating that it should be possible to use damping controls to limit loading in larger seas.

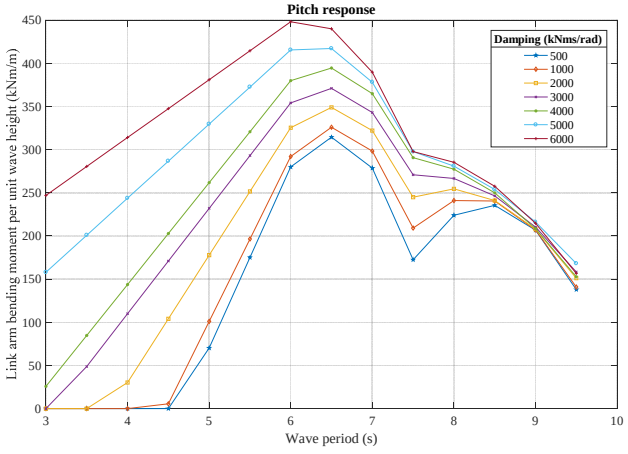

Fig. 15 Pitch response for articulation LA5/S2

The first step in defining a PTO control strategy is to identify appropriate "operational" and "survival" sea states for the device. In the operational state, the machine will be optimised for power extraction. In the survival state, controls will be implemented to facilitate load shedding – no power would be extracted during these sea states.

While the tank testing program was not focussed on extreme storm events it is possible to infer some details about the behaviour of the device in extreme seas from the results. This can then be used as a starting point for defining different machine states that can be developed further during detailed design.

Table VII shows the peak pitch bending moment at the LA5/S2 articulation as measured during the tank tests (with unlimited PTO torque, and damping optimised for maximum power output).

TABLE VIII
Peak Pitch Bending Moment (MNm, Full Scale)– LA5 / S2

H(m) / T(s)	7.7	9.1	9.9	10.5	11.9	12.6	13.3	14.7
4.5				2.17	1.82			
4								
3.5		2.21		1.84			1.28	
3			1.64			1.34		
2.5	1.62		1.45			0.99		
5	1.34	1.33		1.19		0.89		
1.5	1.03	0.97		0.84			0.69	0.51
1	0.75		0.56					

These results have then been interpolated and extrapolated across a full H_s /T_p matrix, up to the theoretical breaking limit, where the wave steepness (wave height / wave length) H/L = 0.14 (Fig. 16).

For wave heights above 4.5m (the highest full-scale wave height encountered during testing), there is a significant amount of uncertainty in the values in Fig. 16, due to the highly non-linear behaviour of waves close to the breaking limit. The results are presented here purely to show the possible loading trend across different sea states when damping is set to maximise power output, and to provide a starting point for the discussion of extreme loads.

H_s/T_p	3	4	5	6	7	8	9	10	11	12	13	14	15	16	17	18	19	20	21
10					4.9	4.7	4.4	4.1	3.7	3.0	2.8	2.6	2.4	2.2	2.2	2.2	1.9	1.6	1.3
9.5					4.7	4.5	4.2	4.0	3.5	2.9	2.7	2.5	2.3	2.2	2.2	2.0	1.7	1.4	1.1
9					4.8	4.3	4.1	3.8	3.4	2.8	2.6	2.4	2.2	2.1	2.1	1.9	1.5	1.2	0.9
8.5					4.9	4.2	3.9	3.6	3.2	2.7	2.5	2.3	2.1	2.1	2.0	1.7	1.4	1.0	0.9
8				5.9	4.9	4.0	3.7	3.5	3.1	2.6	2.4	2.2	2.0	2.0	1.8	1.5	1.2	0.9	1.0
7.5				5.5	4.9	4.0	3.6	3.3	2.9	2.5	2.3	2.1	2.0	1.9	1.6	1.3	1.0	1.0	1.0
7				5.0	4.8	4.0	3.4	3.1	2.8	2.4	2.2	2.0	1.9	1.7	1.4	1.1	1.0	1.0	1.0
6.5				4.4	4.7	3.9	3.3	3.0	2.6	2.2	2.0	1.9	1.8	1.6	1.2	1.0	1.0	1.0	1.0
6				3.9	4.3	3.8	3.2	2.8	2.5	2.1	1.9	1.8	1.7	1.4	1.1	1.0	1.0	1.0	1.0
5.5			3.2	3.4	3.8	3.7	3.1	2.6	2.3	2.0	1.8	1.7	1.5	1.2	1.0	1.0	0.9	0.9	0.9
5			3.0	3.0	3.3	3.5	2.9	2.5	2.2	1.9	1.7	1.6	1.3	1.1	1.0	0.9	0.9	0.9	0.9
4.5			2.7	2.7	2.9	3.1	2.7	2.3	2.0	1.8	1.6	1.4	1.2	1.0	0.9	0.9	0.8	0.7	0.6
4			2.4	2.4	2.5	2.6	2.5	2.1	1.9	1.7	1.5	1.2	1.1	0.9	0.9	0.8	0.7	0.6	0.4
3.5		2.1	2.1	2.1	2.2	2.3	2.2	2.0	1.7	1.6	1.4	1.1	1.0	0.9	0.8	0.7	0.6	0.4	0.3
3		1.9	1.9	1.9	1.9	1.9	1.9	1.6	1.6	1.4	1.1	1.0	0.9	0.7	0.7	0.5	0.4	0.3	0.2
2.5		1.6	1.6	1.6	1.6	1.6	1.6	1.4	1.3	1.1	1.0	0.9	0.7	0.6	0.5	0.4	0.3	0.1	0.0
2	1.6	1.6	1.5	1.4	1.4	1.3	1.3	1.2	1.1	1.0	0.8	0.8	0.6	0.5	0.4	0.2	0.1	0.0	0.0
1.5	1.0	1.0	1.0	1.0	1.0	1.0	1.0	0.9	0.8	0.8	0.7	0.6	0.5	0.3	0.2	0.1	0.0	0.0	0.0
1	1.0	0.9	0.9	0.8	0.8	0.7	0.6	0.5	0.5	0.4	0.4	0.4	0.3	0.2	0.1	0.0	0.0	0.0	0.0
0.5	0.7	0.6	0.6	0.5	0.5	0.4	0.3	0.2	0.2	0.2	0.2	0.2	0.2	0.1	0.0	0.0	0.0	0.0	0.0

Fig. 16 Peak pitch bending moment (MNm, Full Scale) – LA5

In addition to the extrapolation limitation, the torque applied by the PTO mechanism at the articulation points will be physically limited, as discussed in the previous sections, which will alter the extreme loading behaviour. However, it is possible that instantaneous peak loading will be greater than the PTO torque limit due to dynamic effects and other external environmental load actions, therefore for this exercise, any effect of torque limitation has been ignored.

Notwithstanding the limitations with this method, the matrix in Fig. 16 does show that loading increases significantly with increasing wave height and steepness. It is expected that this trend would be further exaggerated due to the non-linear behaviour in steeper seas.

As an initial starting point for definition of the "operational" and "survival" sea states, the link arm steel section required to resist the FLS loading (as calculated in Section III.C) has been checked against different applied extreme link arm bending moments. ULS code based checks have been carried out in accordance with Norsok N-004 [8]. The ULS partial load factor has been taken as 2.6. [4] recommends a load factor of 1.3 for environmental loading, but this has been doubled here to account for the significant amount of uncertainties surrounding the analysis method. The graph in Fig. 17 shows the resulting variation in the utilisation factor (U) with applied bending moment.

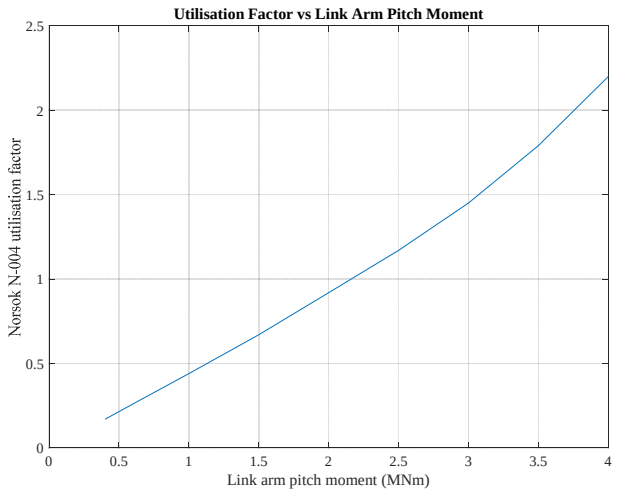

Fig. 17 Utilisation factor vs Link arm Pitch Moment (Full Scale)

This shows that U > 1 for bending moments greater than 2.2MNm. If power production were to take place in sea states where bending moments greater than this value could occur, ULS loading would dominate the design, and the link arm cross sectional area would have to be increased over that required for FLS loading, increasing the overall structural costs and reducing the LCoE.

This criterion has been applied to the bending moments presented in Fig. 16; the sea states where bending moments are greater than 2.2MNm are shown superimposed on the West Harris occurrence matrix shown in Fig. 18, highlighting that they do not occur on a regular basis. If the device was set to be in survival mode during these events to reduce structural loading, this would have a minimal impact on the overall power production capabilities of the device. Using a truncated power matrix, ignoring power generated in the sea states as shown in Fig. 18 reduces the AEP by just 2.5%.

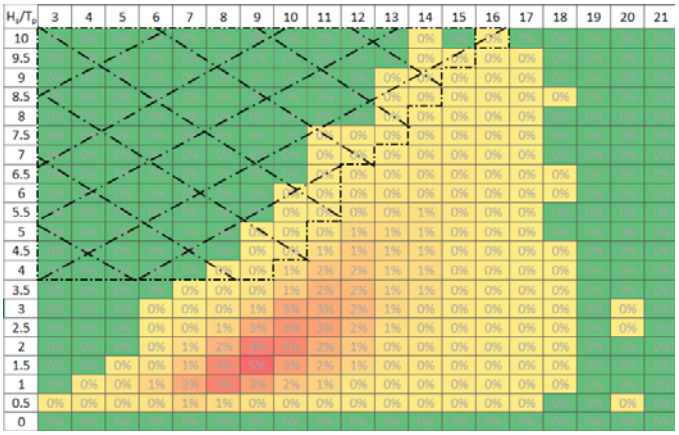

Fig. 18 West Harris Occurrence Matrix. Sea states where ULS requirements > FLS requirements for the design of the link arm are shown in the hatched area. (Illustrative purposes only, due to limitations with extrapolation method for wave heights > 4.5m)

As discussed above, there are significant limitations in extrapolating the link arm bending moments for wave heights greater than 4.5m, due to lack of test data in larger sea states. However, the analysis has been carried out here using the full scatter diagram, as it provides a useful illustration of the proposed methodology. The actual sea states where ULS loading dominates over FLS loading will be revisited once further investigation of the behaviour of the device in extreme seas has been carried out, which may have an impact on the AEP reduction reported above.

However, at this early stage, the analysis indicates that selecting sea states where ULS loading would dominate over FLS loading as a criterion for defining "survival" and "operational" sea states is an appropriate strategy, as it appears to minimise the loss of power production, while reducing the need for larger, more expensive structural components.

VI. Discussion

A. PTO torque limitation

PTO torque limit has a significant impact on power output, structural design, and the cost of many of the components of a wave energy device, and therefore is it beneficial to highlight the optimum torque limit early in the design process. This paper presents a simple method for this using high level concept design methods and early stage tank testing results. In principle, the method is applicable to other technologies, although would need to be adapted to drivers specific to the working principle of a given device.

However, there are certain limitations to the method presented here; for example, the results are very dependent on the chosen site and array configuration. There would be benefit in extending the analysis to check the sensitivity of the results at other sites and array scales, as it would be advantageous to

have a single device design suited to multiple sites and configurations. Also, the analysis only considers the effect of structural costs on LCoE, when other factors (such as the cost of hydraulic and electrical components) will also have an impact. At this stage, it is assumed that these other factors will follow the same trends as the structural costs, however it will be important to check that this is still valid as the design progresses.

B. PTO damping control and machine state definition

As the tank testing focussed on the behaviour of the device during operational sea states, the validity of the analysis carried out for the ULS loading is limited by the method of extrapolation into non-linear sea states. However, the benefit of the work presented here is that it sets out an approach to determine ULS and FLS dominated regions, which can be used to define appropriate "operational" and "survival" sea states. It is valuable to carry this out at an early stage, as it feeds into the development of the PTO design and control strategy, which will need to define appropriate damping settings to allow for maximum power generation in the smaller "operational" seas, and load shedding in larger "survival" seas.

VII. CONCLUSIONS

This paper has investigated the relationship between power output and structural loading, looking at the effect of the PTO torque limit on operational loads, and PTO damping controls on extreme loads.

From this work the following conclusions can be drawn:

- The selected PTO torque limit has a significant effect on the fatigue damage accumulated during the lifetime of the device.
- While structural costs continuously increase with increasing PTO torque, the rate of change slows with increasing torque limit. This is because lower torque limits have a greater impact on the amount of fatigue cycles that the device is subject to than higher limits.
- A PTO limit of 0.8MNm gives the lowest value of LCoE, and therefore this should be taken forward as a starting point for the detailed design of the PTO mechanism for the identified site.
- Reduction in PTO damping reduces structural loading, and therefore it can inform a "survival" control strategy to limit structural loading during extreme sea states
- Defining "survival" sea states as those where ULS loading would dominate over FLS loading (which is driven by the "operational" sea states) appears to have a minimal effect on power output, while reducing the need for larger, more expensive structural components. Therefore, this could be an appropriate strategy to adopt for defining the different machine states.

VIII. FURTHER WORK

This work uses results from tank testing, which provides detailed information about the behaviour of the device during a limited amount of sea states. The next step in this work is to use the tank testing results to validate the numerical models used for design. These models can then be used to give detailed information about the behaviour in sea states that were not tested, to reduce the uncertainties associated with the interpolation and extrapolation of the tank testing results.

Further testing programmes would also be beneficial to focus on the behaviour of the device during extreme events, and to study the impact of different damping control strategies and torque limitation.

ACKNOWLEDGMENT

This work has been carried out using tank test data with the permission of Albatern Wave Energy. The analysis presented in this paper builds on work carried out by other members of the Albatern team, in particular Vivien Mavel and Anthony McDonald who ran the testing programme and carried out the initial data processing and analysis, and Ciaran Frost who developed the LCoE modelling tool.

Tank testing was funded by Wave Energy Scotland (WES) as part of the Novel Wave Energy Converter Stage 1 (NWEC1) programme.

This work has been carried out as part of the IDCORE programme, funded by the Energy Technology Institute and RCUK Energy programme (grant no. EP/J500847/1)

REFERENCES

[1] B. Holmes, *Tank Testing of Wave Energy Conversion Systems*, Marine Renewable Energy Guides, EMEC, 2009

[2] *Design of Offshore Steel Structures, General (LRFD Method)*, DNV Offshore Standard, DNV-OS-C101, 2014.

[3] DNV, *Guidelines on Design and Operations of Wave Energy Converters*, Carbon Trust, 2005.

[4] *Fatigue Design of Offshore Steel Structures*, DNV Recommended Practice, DNV-RP-C203, 2011.

[5] J. Schijve, *Fatigue of Structures and Materials*, Springer, 2009.

[6] A. Nieslony, *rainflow.m*, matlab function, Available: http://uk.mathworks.com/matlabcentral/fileexchange/3026-rainflow-counting-algorithm

[7] (2017) Interfluid Hydraulics Ltd website. [Online] Available: https://interfluid.co.uk/store/

[8] *Design of Steel Structures*, NORSOK Standard N-004, rev 3, 2013.